

# Electrons in finite superlattices: the birth of crystal momentum

P. Pfeffer\* and W. Zawadzki  
*Institute of Physics, Polish Academy of Sciences*  
*Al.Lotnikow 32/46, 02-668 Warsaw, Poland*

(Dated: December 17, 2020)

Properties of electrons in superlattices (SLs) of a finite length are described using standing waves resulting from the fixed boundary conditions (FBCs) at both ends. These electron properties are compared with those predicted by the standard treatments using running waves (Bloch states) resulting from the cyclic boundary conditions (CBCs). It is shown that, while the total number of eigenenergies in a miniband is the same according to both treatments, the number of *different* energies is twice higher according to the FBCs. It is also shown that the wave vector values corresponding to the eigenenergies are spaced twice as densely for the FBCs as for the CBCs. The reason is that a running wave is characterized by a single value of wave vector  $k$ , while a standing wave in a finite SL is characterized by a pair of wavevectors  $\pm q$ . Using numerical solutions of the Schrodinger equation for an electron in an increasing number  $N$  of periodic quantum wells (beginning with  $N = 2$ ) we investigate the "birth" of an energy miniband and of a Brillouin zone according to the two approaches. Using the Fourier transforms of the computed wave functions for a few quantum wells we follow the "birth" of electron's momentum. It turns out that the latter can be discerned already for a system of *two* wells. We show that the number of higher values of the wave vector  $q$  involved in an eigenenergy state is twice higher for a standing wave with FBCs than for a corresponding Bloch state. Experiments using photons and phonons are proposed to observe the described properties of electrons in finite superlattices.

PACS numbers: 73.20.At 73.21.Cd 73.21.Fg

## I. INTRODUCTION

Semiconductor superlattices (SLs) have been, since their creation in the early seventies [1], a subject of intensive studies because of their inherent scientific interest as well as important applications. Together with other heterostructures, SLs belong to "hand made" quantum systems which can be used to study fundamental features of quantum mechanics. In particular, SLs are good examples of periodic or quasiperiodic structures exhibiting quantum effects of periodicity. From their beginning, SLs have been treated theoretically by methods developed earlier for atomic crystals. Thus, the standard notions of Bloch functions, energy bands, forbidden gaps, crystal momenta, Brillouin zones, etc., have been used for their description, see [2]. It is true that a SL and an atomic crystal exhibit many similarities. The main practical difference between them is that a typical crystal contains millions of unit cells, while a one-dimensional SL may contain only tens or hundreds of quantum wells (QWs). This means that the usually imposed cyclic boundary conditions (CBCs) apply much better to an atomic crystal than to a SL. Also, the notions of continuous energy bands and wave vector spaces apply much better to a crystal than to a SL.

The purpose of our present work is threefold. First, we explore to what extent the notions taken from "infinite" atomic crystals apply to finite superlattices. In

particular, we focus on periodic systems consisting of a few quantum wells and analyze how the features characteristic of long periodic systems are "formed" as the number of QWs increases. Second, we work out specific features of electrons in finite SLs and, third, we propose experiments to observe them. The essential point of our approach is that we realistically consider a finite superlattice to be a quantum well. Concentrating on important features we consider only the ground energy miniband, we do not treat higher minibands and states in energy gaps.

The paper is organized as follows. In Section II we review very briefly properties of "infinite" superlattices (or crystals) with imposed CBCs. Next we consider theoretically various aspects of finite SLs. Finally, we discuss our results and propose experiments to observe the described new features. The paper is concluded by a summary.

## II. "INFINITE" SUPERLATTICES WITH CYCLIC BOUNDARY CONDITIONS

In this section we consider very briefly "infinite" superlattices and crystals using CBCs. Since electrons in "infinite" crystals are described in many textbooks, we only emphasize their main features treating them as a starting point for our main considerations. An "infinite" sequence of quantum wells is sketched schematically in Fig. 1, which also indicates parameters of the SL rectangular potential. The potential energy  $V(z)$  is a periodic

---

\* e-mail address: pfeff@ifpan.edu.pl

function of  $z$  with the period  $d$ :

$$V_{SL}(z) = \sum_{l=-\infty}^{+\infty} V(z - ld) , \quad (1)$$

in which

$$V(z - ld) = \begin{cases} -V_b & \text{if } |z - ld| \leq a/2 \\ 0 & \text{if } |z - ld| > a/2 \end{cases} .$$

The zero of energy is taken at the barrier's height. Exploiting the periodicity of  $V_{SL}(z)$  one considers the translation operator  $\tau$  which is such that for any function  $f(z)$  there is  $\tau f(z) = f(z+d)$ . The operator  $\tau$  commutes with the Hamiltonian  $H$  of the electron because of the periodicity of  $V(z)$ . One can thus find the eigenfunctions of  $H$  which are simultaneously the eigenfunctions of  $\tau$ . These common eigenfunctions are the Bloch states

$$\chi_k(z) = e^{ikz} u_k(z) , \quad (2)$$

in which  $u_k(z)$  is a periodic function possessing the periodicity of the potential. It is usually assumed that the length of the crystal  $L = Nd$  is very large and one can impose the cyclic Born-von Karman boundary conditions on the eigenstates of  $H$ . Then  $\chi_k(z)$  obey

$$\chi_k(z + Nd) = \chi_k(z) , \quad (3)$$

which, upon the periodicity of  $u_k(z)$ , gives:  $e^{ik(z+Nd)} = e^{ikz}$ , so that  $e^{(ikNd)} = 1$ , and the well known quantization of  $k$  is obtained

$$k_j = \frac{2\pi j}{Nd} = \frac{2\pi}{L} j , \quad (4)$$

where  $j = 0, 1, 2, \dots, N$ . There are  $N$  independent values of  $j$ , the spacing between any two consecutive  $k$  values being  $2\pi/L$ . For  $j = N$  we have  $k_N = 2\pi/d$ . Without loss of generality one may restrict  $k$  to the range  $[-\pi/d, +\pi/d]$  which is called the first Brillouin zone (BZ). Then  $j = 0, \pm 1, \pm 2, \dots, \pm N/2$ . The quantity  $\hbar k$  is called crystal momentum, for the  $k$  values within the first BZ it plays the role of momentum. If a crystal lattice is characterized by an inversion symmetry, the electron waves with  $k$  and  $-k$  are equivalent and the energy has the property  $\mathcal{E}(-k) = \mathcal{E}(k)$ , see e.g. [3]. Thus each energy in a Brillouin zone has a double degeneracy (without spin). One proves that  $\mathcal{E}(k)$  relation for a given band is periodic in the  $k$  space: the  $\mathcal{E}(k)$  relation in the first BZ  $[-\pi/d, +\pi/d]$  is repeated in the second BZ  $[+\pi/d, +3\pi/d]$ , etc., and similarly for the negative  $k$  values, see below.

Two remarks are in order. First, the precise values of  $k_j$  (including  $k_0 = 0$ ) are allowed because the electron in an "infinite" crystal is completely delocalized, so its momentum may be given exactly. Second, it is seen from Eq. (2) that the Bloch states represent running waves. Again,

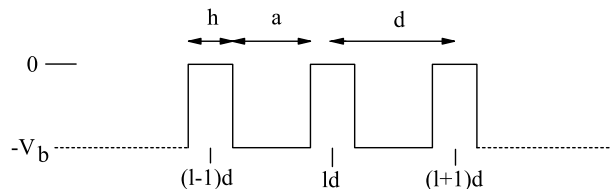


FIG. 1: Rectangular periodic potential of a superlattice used in the calculations: a) Imposing cyclic boundary conditions, see Eq. (3); b) Imposing fixed boundary conditions in the presence of thick barriers at both ends, see Eq. (6).

this is possible because the crystal is assumed to be infinite, so the electron can propagate in one direction and does not bounce back. For an "infinite" rectangular SL the solution of the one-dimensional Schroedinger equation is known exactly for both well-acting and barrier-acting layers. If the electron effective mass is the same in the wells and in barriers (which is an idealization) both the wave function and its derivative must be continuous at the two inequivalent interfaces. Using these boundary conditions one obtains four equations from which a relation between the wave vector  $k$  and the energy  $\mathcal{E}$  is obtained in the form (cf. [4], [5])

$$\begin{aligned} \cos(k_j d) &= \cos(k_w a) \cosh(\kappa_b h) + \\ &- \frac{1}{2} \left[ \frac{-\kappa_b}{k_w} - \frac{k_w}{\kappa_b} \right] \sin(k_w a) \sinh(\kappa_b h) , \end{aligned} \quad (5)$$

where  $\kappa_b = \sqrt{-2m^* \mathcal{E} / \hbar^2}$ ,  $k_w = \sqrt{2m^* (\mathcal{E} + V_b) / \hbar^2}$ . Relation (5) is valid for the energies  $-V_b \leq \mathcal{E}(k_j) \leq 0$ . In the limit of very thick barriers the RHS of Eq. (5) goes over to the  $\mathcal{E}(k)$  relation for a single well. Equation (5) gives all energy levels  $\mathcal{E}(k_j)$  corresponding to both even and odd states. The energy minibands of negative energies result from a hybridization of isolated well states due to coupling across finite barriers. The energies  $\mathcal{E}(k_j)$  calculated from Eq. (5) for the ground energy miniband are quoted below.

### III. FINITE SUPERLATTICES

We now turn to our main considerations regarding the electron behavior in finite superlattices. In order to concentrate on main features we take a simple rectangular potential, similar to the one shown in Fig. 1, and assume again that the electron effective mass is the same in the wells and in barriers. The essential new feature is that the SL is made finite by putting thick barriers on its both sides having the same height as the barriers between quantum wells (QWs). The total length of our SL is  $L = Nd$ . We intend to compare the resulting electron properties with those mentioned in the previous section for "infinite" SL. For a finite superlattice we are not able to derive analytical results, so our conclusions

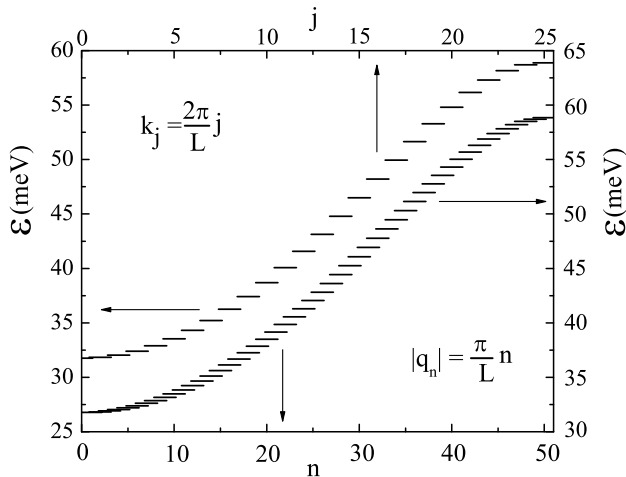


FIG. 2: Theoretical ground energy miniband of a superlattice consisting of  $N = 50$  QWs. Upper trace: result of standard calculation based on CBCs and running waves [see Eq.(5)]. The other half of the miniband corresponds to negative  $j$  values (not shown). Lower trace: result of present calculation based on FBCs and standing waves. The upper trace is shifted 5 meV upwards for clarity. The values of wave vectors in the two cases are indicated by the formulas.

will be mostly illustrated by numerical calculations. In all our computations we use the values  $a = 8$  nm,  $h = 2$  nm,  $d = 10$  nm,  $V_B = 240$  meV (see Fig. 1), and the effective mass  $m^* = 0.067 m_0$  (the same for the wells and barriers). The considered structure is characterized by the inversion symmetry. The Schrodinger equation is solved numerically using the potential shown in Fig. 1, for a given number  $N$  of QWs. The boundary conditions at each interface assure the continuity of the wave function and its derivative.

As to the electron behavior, there exist essential differences between the standard model of an "infinite" crystal (or superlattice) and our finite superlattice. First, in our case *the potential is not periodic* because at each point  $z$  the distances from both ends vary. Second, in our case the electron wave function may *not* be represented by a *running wave* [see Eq. (2)], but it must be a *standing wave* of some sort, characteristic of a finite height quantum well. In classical terms, in an infinite periodic structure the electron with the crystal momentum  $\hbar k$  (or  $-\hbar k$ ) runs indefinitely in one (or the other) direction without coming back. In a finite structure it bounces back and forth which means that in each state both  $\hbar q$  and  $-\hbar q$  values are simultaneously involved. Third, since in a finite SL the electron is confined to a length of about  $L$ , the value of its *momentum may not be precisely given* because of the uncertainly principle. Since  $\Delta z \approx L$  the uncertainly  $\Delta p$  must go as  $1/L$ . Numerical calculations confirm this result, see below.

We first consider eigenvalues of the energy which, in contrast to momentum, is a good quantum number for our system. Figure 2 shows the computed electron energies in the ground miniband for a SL of  $N = 50$  QWs. These eigenenergies are compared with those calculated

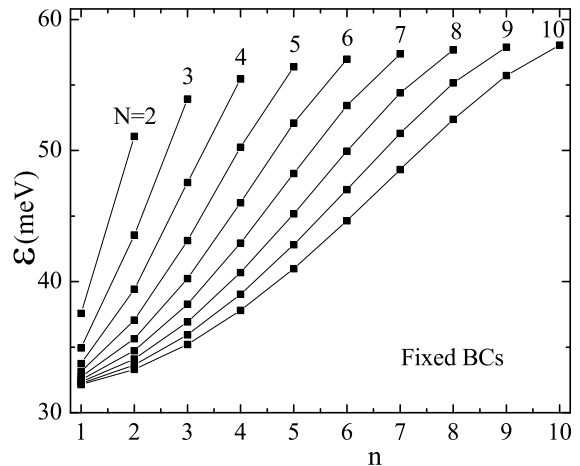


FIG. 3: Low energies of electrons in SLs with increasing number  $N$  of QWs versus wave vector  $n$  (in  $\pi/L$  units), as calculated using fixed BCs. A formation of s-like shape of a miniband is seen. The lines join the points to guide the eye.

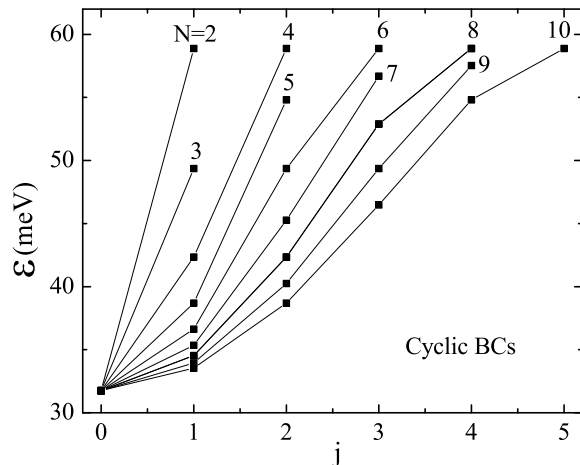


FIG. 4: Low energies of electrons in SLs with increasing number  $N$  of QWs versus wave vector  $j$  (in  $2\pi/L$  units), as calculated using cyclic BCs. A formation of s-like shape of a miniband is seen. The lines join the points to guide the eye.

from Eq. (5) for an SL with the cyclic boundary condition for  $N = 50$ . It is seen that one obtains in both cases a similar ground miniband with the same energy width. Also, the *total* number of allowed energies is the same. On the other hand, the number of *different* allowed energies for a finite SL is *twice* that for an SL with CBCs and it is equal to the number of QWs. This is due to the fact that for an "infinite" SL each energy is twice degenerate with respect to  $k$  and  $-k$ , while for a finite SL this degeneracy does not occur. This result is in agreement with the well known fact that for two QWs the energies of the symmetric and odd electron states are not the same. A closer inspection of Fig. 2 indicates that, for a finite SL, one does not deal with split doublets of the degenerate energies. Instead, the energies are distributed rather uniformly.

Now we estimate quantized values of the quantity  $q$  (we hesitate as yet to call it crystal momentum). The

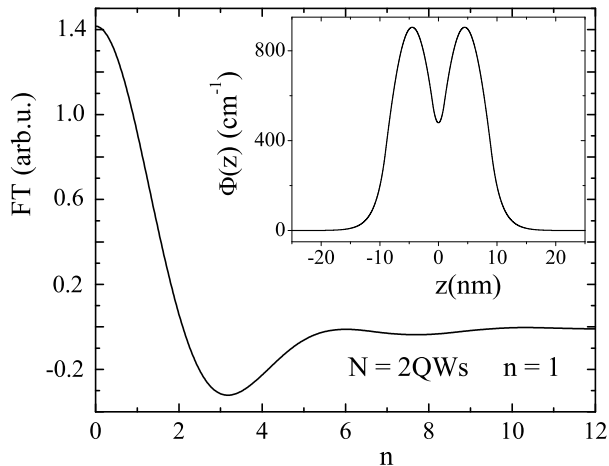


FIG. 5: Calculated Fourier transform of the even wave function (lower energy state,  $n = 1$ ) for  $N = 2$  QWs versus wave vector  $n$  (in  $\pi/L$  units). The wave function is shown in the inset.

wave functions in a finite SL are standing waves, they should satisfy the following approximate fixed boundary conditions (FBCs)

$$\Psi(-L/2) = \Psi(L/2) \approx 0. \quad (6)$$

In principle, our problem is that of an electron in a finite-height rectangular well but for simplicity we will approximate it by considering an infinitely high rectangular well. Then the eigenfunctions are either  $\Psi(z) = A\cos(qz)$  (even states), or  $\Psi(z) = B\sin(qz)$  (odd states). The FBCs for the cosine function give  $qL = (1 + 2r)\pi$ , where  $r = 0, \pm 1, \pm 2, \dots$ , while the FBCs for the sine function give  $qL = 2r\pi$ , where  $r = \pm 1, \pm 2, \dots$ . The above conditions may be combined into a simple equation

$$|q_n| = \frac{\pi}{L}n, \quad n = 1, 2, 3, \dots \quad (7)$$

It is seen that the values of  $q_n$ , as given by Eq. (7) for a finite SL and resulting from FBCs, are spaced *twice as densely* as those for an "infinite" structure according to CBCs. Still, the total number of wave vector states in both cases is the same and is equal to  $N$ . The difference is that for CBCs the states correspond to *single*  $k$  values:  $k = (2\pi/L)(-N/2), \dots, (2\pi/L)(N/2)$ , while for FBCs the states correspond to *pairs* of values:  $q = \pm(\pi/L)1, \dots, \pm(\pi/L)N$ .

The energies  $\mathcal{E}$  for "infinite" and finite SLs are plotted as functions of  $j$  and  $n$  in Fig. 2. According to the above considerations, the upper trace in Fig. 2 describes half of the BZ according to CBCs (the other half is given by  $-25 \leq j \leq 0$ ), while the lower trace corresponds to the complete BZ according to FBCs. We emphasize again that the relation (7) is approximate, as it has been obtained from the consideration of an infinitely high rectangular well. We come back to this point below. It should be noted that the CBCs allow for  $k_0 = 0$ , while for the FBCs the value  $q = 0$  is not allowed, see the discussion below.

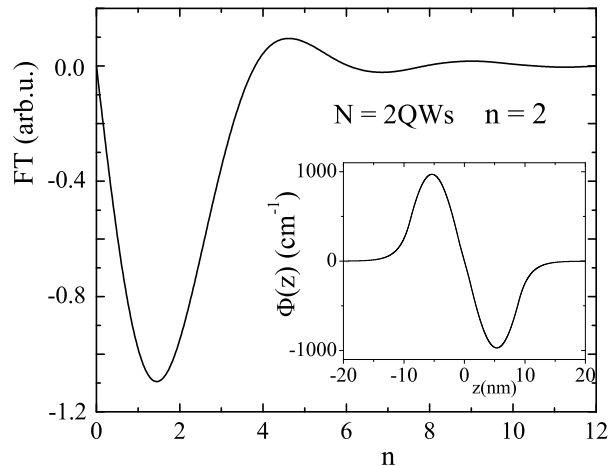


FIG. 6: Calculated Fourier transform of the odd wave function (upper energy state,  $n = 2$ ) for  $N = 2$  QWs versus wave vector  $n$  (in  $\pi/L$  units). Strong peak below  $n = 2$  is seen. The wave function is shown in the inset.

A one-dimensional density of states in the energy space is  $\rho(\mathcal{E}) \sim dk/d\mathcal{E}$ . It is clear that, if  $\rho(\mathcal{E})$  is considered in an energy range including many levels, it will be similar (if not identical) in both cases because the  $\mathcal{E}(k)$  and  $\mathcal{E}(q)$  relations are similar. However, if one is interested in  $\rho(\mathcal{E})$  on the scale of one or two levels, the two cases will give considerably different results.

It is of interest to study how the energy band shown in Fig. 2 is formed. We consider it first for the FBCs. Clearly, for one QW one can not have a band since there is no periodicity. For two QWs, the two lowest energies (resulting from the above mentioned splitting related to the even and odd states) already form a "germ" of the ground energy band. When more QWs are added, the energies gradually develop into a real band. This process is illustrated in Fig. 3, in which we show the calculated energies for nine SLs consisting of  $N = 2$  to  $N = 10$  QWs. It is seen that, beginning with  $N = 4$ , the energy values  $\mathcal{E}(q_n)$  form the characteristic s-like shape of an energy band. It is also seen that the width of the ground energy band  $\Delta\mathcal{E}$  increases with increasing  $N$ . However, the width  $\Delta\mathcal{E}$  quickly saturates, so that for  $N = 10$  it almost reaches its final value. Thus for  $N = 10$  the energy width shown in Fig. 3 is 25.9 meV, while the width shown in Fig. 2 for  $N = 50$  is 27.06 meV.

Also, Fig. 3 partially elucidates a formation of the Brillouin zone. One can define a Brillouin zone in various ways, the simplest would be to say that a BZ is well formed if the  $\mathcal{E}(q_n)$  relation is horizontal at the point  $|q_N| = \pi NL = \pi/d$ , so that the electron velocity vanishes at this point:  $v = (d\mathcal{E}/d\hbar q)_{q_N} \approx 0$ . It is seen from Fig. 3 that, according to this criterion, even for  $N = 10$  the dependence  $\mathcal{E}(q_n)$  is not horizontal at  $q_{10}$ . In other words, a SL of 10 QWs is not "periodic enough" to form a good Brillouin zone.

Now we consider the same problems according to the CBCs, i.e. using Eq. (5) for the eigenenergies. This approach is clearly not good for few QWs but we try it

anyway in order to expose its limitations. The results are shown in Fig. 4 for an increasing number  $N$  of QWs. It follows from Fig. 4 that for the extreme case of  $N = 2$ , the model gives *three* energies:  $\mathcal{E}_{\pm 1}$  and  $\mathcal{E}_0$ . The last one could be considered as an artefact but, interestingly, the energy difference  $\mathcal{E}_1 - \mathcal{E}_0$  gives the exact width of the miniband reached at high values of  $N$ . It is seen that, for even  $N$  values, the number of eigenenergies is  $N + 1$  and the miniband width is always the same. For  $N = 3$  there are also three eigenenergies:  $\mathcal{E}_{\pm 1}$  and  $\mathcal{E}_0$ . For odd  $N$  values the number of eigenenergies is always  $N$  and the width of a miniband increases with  $N$ . In that sense the model of CBCs is more "natural" for odd  $N$  values. As expected, the exact calculation for a few QWs with the use of FBCs is distinctly better than that using CBCs, while for high  $N$  values the two models give similar minibands, as illustrated in Fig. 2.

Finally, we consider the problem of whether the electron in a finite SL can be characterized by a crystal momentum. To put the question differently: how many periodic quantum wells does one need to be able to talk of the crystal momentum? Trying to answer this question with the use of FBCs we first compute the wave functions corresponding to specific eigenenergies and then calculate their Fourier spectra to see what values of the wave vector are involved in them. It is clear without any calculations that, since we are dealing with standing waves and the system is characterized by the inversion symmetry, the Fourier transforms (FTs) must be symmetric in  $q$  and  $-q$ . To be more specific, we begin with a SL of  $N = 2$  and calculate the wave functions corresponding to the eigenenergies shown in Fig. 3. The lowest state is even ( $n = 1$ ) and the higher state is odd ( $n = 2$ ). Their FTs are shown in Figs. 5 and 6. For  $n = 1$  the maximum of FT is at  $q_1 = 0$ . This result is not reasonable because one expects the maximum to be near  $|q_1| = 1$  (in  $\pi/L$  units). The reason is that for  $n = 1$  the corresponding wavelength is  $\lambda_1 = 2\pi/q_1 = 2L$ . Since the length of our SL is  $L$ , it follows that for  $n = 1$  only half of the full wavelength fits into the SL. It is known that one needs at least one full wavelength to fit into the considered length to make the Fourier analysis meaningful. This is the case for  $n = 2$ , because  $\lambda_2 = 2\pi/q_2 = L$ , so that one full wavelength fits into the SL. It is seen from Fig. 5 that the FT for the upper energy state has a pronounced extremum below  $n = 2$ .

The above results merit some comments. First, the reasoning for  $n = 1$  is equally valid for any  $N$ , so that also for longer SLs the FTs for  $n = 1$  are not meaningful. Our calculations confirm this conclusion. Second, it is seen that, as expected, the main peak has a finite width  $\Delta n$ . Still, anticipating a little we can say that already for  $N = 2$  the electron motion in the state  $n = 2$  is dominated by a specific value of crystal momentum (positive and negative).

Clearly, SLs with higher number of QWs possess a better pronounced periodicity. In the insets of Figs. 7, 8 and 9 we show, as a matter of example, calculated wave func-

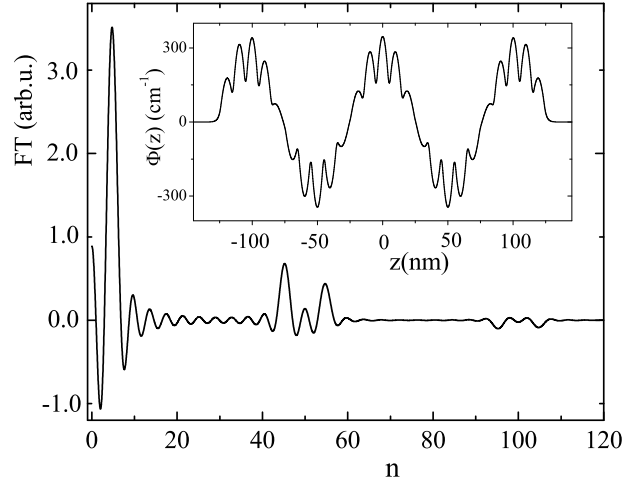


FIG. 7: Calculated Fourier transform of the wave function (shown in the inset) for  $N = 25$  QWs and  $n = 5$  versus wave vector  $n$  (in  $\pi/L$  units). The basic peak just below  $n = 5$  and high- $n$  peaks are seen. The wave function is a product of the envelope (standing wave) and the periodic component.

tions corresponding to the eigenenergies  $\mathcal{E}_n$  for SLs of  $N = 25, 50$  and  $100$  QWs, respectively. They resemble the Bloch states by having quickly oscillating periodic components and slowly varying envelopes. Still, in true Bloch states the envelope functions are running waves  $\exp(\pm ikz)$ , while in our case the envelope functions are standing waves of  $\sin(qz)$  and  $\cos(qz)$  type.

The Fourier transforms of the above wave functions are shown in Figs. 7, 8 and 9, they indicate what crystal momenta are involved in the corresponding electron motion. We first consider Fig. 7. It is seen that we deal with a pronounced peak corresponding approximately to the "main" value of crystal momentum  $n = 5$ . The peak has the width of  $\Delta n \approx 4$ . Since the SL has the length  $L \approx \Delta z$ , it follows that  $\Delta z \cdot \hbar \Delta q \approx L \hbar 4\pi/L = 4\pi\hbar$ . Thus the width  $\Delta q$  is directly related to the uncertainty principle. Our calculations for SLs of different numbers  $N$  show that the main peak has always about the same width  $\Delta n \approx 4$ . The corresponding width  $\Delta q \approx 4\pi/L$ , so that the uncertainty of momentum decreases when the length of SL increases. This means that for really long SLs the main FT peak approaches the Dirac  $\delta$ -function. We emphasize again that the complete Fourier transforms contain not only the functions shown in Figs. 6, 7, 8 and 9 but also their mirror images for negative  $n$  (and  $q$ ).

The remarkable feature seen in the FTs shown in Figs. 7, 8 and 9 are additional sharp peaks at higher  $n$  values. In Fig. 7, in addition to the main peak near  $n = 5$ , there are peaks at  $n = 45, 55, 95, 105, \dots$ . In Fig. 8, the main peak is near  $n = 10$ , the additional peaks occur at  $n = 90, 110, 190, 210, \dots$ . The origin of the additional peaks is understood when one recalls the fact well known from the theory of infinite periodic systems, that the  $\mathcal{E}(k)$

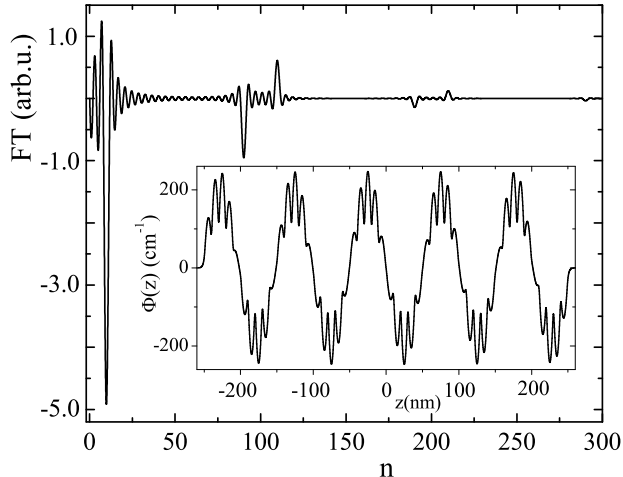


FIG. 8: The same as in Fig. 7, but for  $N = 50$  QWs and  $n = 10$ . The basic peak just below  $n = 10$  and high- $n$  peaks are seen.

relation for each energy band is a periodic function of  $k$  (see e.g. Ref. 3). We plot schematically a similar function for a finite SL, see Fig. 10. It is seen that a given value of the energy corresponds to many possible values of  $n$  (or  $q$ ) and the additional peaks occur exactly at these  $n$  values. We demonstrate this rule considering the results shown in Fig. 7. The main peak is at  $n_1 = 5$  and the edge of the BZ is at  $N = 25$ . According to Fig. 10 the horizontal line at the energy  $\mathcal{E}(n_1)$  crosses the  $\mathcal{E}(n)$  dependence first at  $n_2 = N - n_1 + N = 45$ , then at  $n_3 = 2N + n_1 = 55$  etc, in agreement with the above values. This result can be simply interpreted recalling that to a given eigenenergy  $\mathcal{E}_n$  there always corresponds predominantly a pair of  $-q_n$  and  $+q_n$  wave vectors in the first BZ. Then the additional peaks are simply repetitions of the above fundamental pair in the second BZ, third BZ, etc. Not knowing anything about the theory of periodic structures but only regarding the function shown in Fig. 7, one would expect its FT to reflect a long wavelength (low  $n$ ) due to the envelope and a short wavelength (high  $n$ ) due to the periodic component. The latter contains 25 oscillations in Fig. 7, 50 oscillations in Fig. 8, and 100 oscillations in Fig. 9. What one finds in Figs. 7, 8 and 9 are the expected main peaks at  $n_1$ , while the high- $n$  peaks are combinations of  $N$  with  $n_1$ . Comparing heights of the main and high- $n$  peaks in Figs. 6, 7, 8, 9 one sees that they increase with  $N$  and the peaks resemble more and more the  $\delta$ -functions. The reason is that in longer SLs the electrons are less localized and their momenta can be specified with greater precision. Also, with increasing  $N$  the main peaks coincide better with the corresponding values of  $n$ . It is because of this coincidence that we could associate the eigenenergies with specific values of  $n$  in Fig. 2. All in all, our considerations of the FTs can be summarized as follows: 1) the

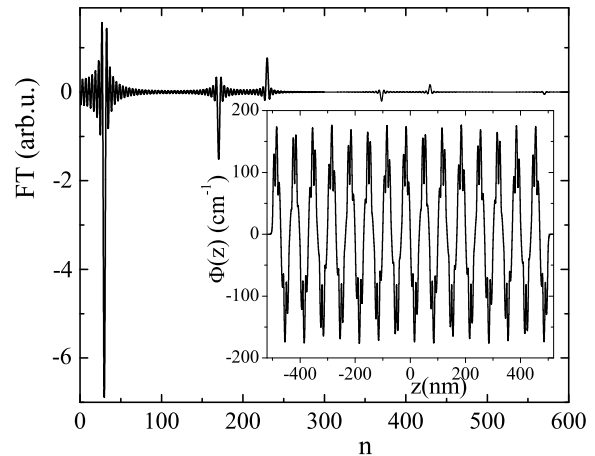


FIG. 9: The same as in Figs. 7 and 8, but for  $N = 100$  QWs and  $n = 30$ . The basic peak at  $n = 30$  and high- $n$  peaks are seen.

main  $n$  peaks are broadened because we deal with finite-length SLs, 2) high- $n$  peaks reflect the periodicity of the structure. To this we want to add an important comment that finite SLs are *not* characterized by an equivalence of states with the wavevectors  $q$  and  $q + G_i$ , where  $G_i$  is the reciprocal lattice vector. This follows from Figs. 7, 8 and 9, where the main  $q$  peaks are much higher than others.

We can interpret the high- $n$  peaks in the FTs of electron states by recalling a well known property of the Bloch functions for "infinite" periodic structures [6]. If a Bloch state  $\Psi$  contains a certain wave vector  $k_0$ , all the wave vectors in the Fourier expansion of this state are given by  $k_0 + G_i$ , where  $G_i$  are the reciprocal lattice vectors. The FTs shown in Figs. 7, 8 and 9 exhibit exactly this property. The difference compared to the standard theory is, that a Bloch state is characterized by *one* value  $k_0$ , whereas our states are characterized by a *pair* of values  $\pm k_0$ . In consequence, each value gives rise to a series:  $+k_0 + G_i$  and  $-k_0 + G_i$ , and we deal with twice as many high- $n$  peaks compared to the standard Bloch states. One can also say that the high- $n$  peaks, corresponding to the descending parts of the  $\mathcal{E}(n)$  curve (peak  $n_2$  in Fig. 10), provide evidence for the mirror-image parts of FTs (with negative  $n$ ) which we do not show in our figures.

We conclude this section by two remarks of a more general nature. First, as follows from a comparison of Eq. (7) with Eq. (4) and of Fig. 3 with Fig. 4, the model of CBCs allows for the value of wave vector  $k = 0$ , while our realistic calculation for finite SLs with the use of FBCs does not allow this value, the smallest  $q$  being  $\pm 1$ . The last result is a direct consequence of the uncertainty principle. However, it means that, while according to CBCs the electron can be at rest, in a real finite periodic structure the electron may not be at rest and we deal with a kind of "zero point oscillations" for the crystal momentum. Second, it follows from the above considerations

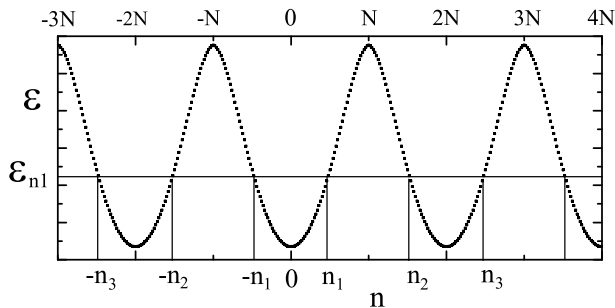


FIG. 10: Periodic  $\mathcal{E}(n)$  function of the ground energy miniband for a SL of  $N = 50$  QWs versus  $n$  (schematically). Constant-energy line  $\mathcal{E}_{n1}$  intersects the  $\mathcal{E}(n)$  curve in consecutive Brillouin zones, which determines the high- $n$  components involved in the wave function.

that in a finite unperturbed periodic structure the electron always bounces back and forth, while according to the cyclic BCs it propagates in one direction. The question arises how to reconcile the two treatments when the structure is long. This can be done introducing scattering events. If the electron scatters from time to time, it will not bounce back and forth. In other words, if the mean free path  $l$  is shorter than the SL length  $L$ , a standing wave is equivalent to a running wave. This justifies the common use of Bloch states in the scattering theory.

#### IV. EXPERIMENTAL POSSIBILITIES

It appears that experimental observations of characteristic electron properties in finite SLs should not be too difficult. As we showed above, the number of *different* eigenenergies in a miniband doubles compared to that in an "infinite" SL described by the CBCs, see Fig. 2. This corresponds to distinctly smaller energy differences between consecutive eigenstates in a miniband. These energy differences can be directly observed by infrared optical absorption. A photon carries almost no momentum, so that, if consecutive states were characterized by sharp different values of the wave vector  $q_n$ , optical transitions between them would not be possible. However, as we argued above, the energy eigenstates are characterized by somewhat spread-out  $q$  values, so the optical transitions with  $q$  conservation are possible. It is clear that for longer SLs, which are characterized by a "better" periodicity, such optical transitions have a lower probability.

We calculated the matrix elements for optical transitions in the electric dipole approximation. The Hamiltonian for the electron-photon interaction is:  $H' = (e/m^*c)\mathbf{A}' \cdot \mathbf{p}$ , where  $\mathbf{A}'$  is the vector potential of radiation. Thus the matrix elements for optical transitions are  $\langle \Psi_f | \mathbf{p} | \Psi_i \rangle$ , where  $i$  and  $f$  subscripts stand for the initial and final electron states, respectively. We computed numerically the matrix elements  $\langle \Psi_2 | (d\Psi_1/dz) \rangle$  and  $\langle \Psi_4 | (d\Psi_1/dz) \rangle$  using the electron wave functions of the type shown in Figs. 7, 8 and 9. The results are

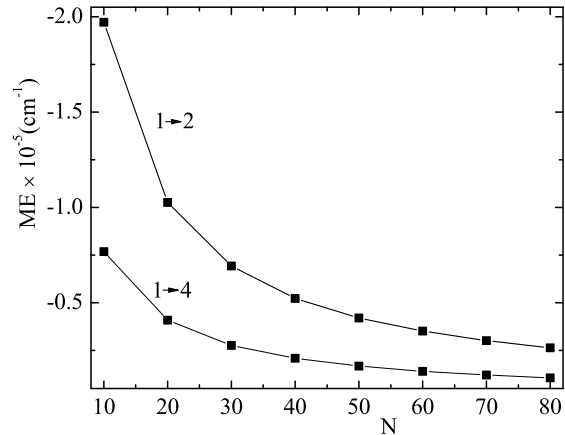


FIG. 11: Matrix elements for optical transitions between 1 $\rightarrow$ 2 and 1 $\rightarrow$ 4 states, calculated for SLs with increasing number  $N$  of QWs. The lines join the points to guide the eye.

shown in Fig. 11 for SLs consisting of  $N = 10$  to  $N = 80$  QWs. It is seen that, in agreement with the above considerations, the MEs decrease when  $N$  increases. Also, the MEs for 1 $\rightarrow$ 4 transitions are considerably smaller than those for 1 $\rightarrow$ 2 transitions because the overlap of  $q$  values is much smaller for the former. The MEs for odd $\rightarrow$ odd and even $\rightarrow$ even transitions vanish since the corresponding wave functions have the same parity.

In order to get an idea about the absolute values of the MEs we compare them with that for the cyclotron resonance. The ME for a transition between the zeroth and first Landau levels is  $\hbar/L_m$ , where  $L_m = (\hbar/eB)^{1/2}$  is the magnetic radius. Since in MEs given in Fig. 11 we omitted  $\hbar$ , we have to compare their values with  $1/L_m$ . For  $B = 4$  Tesla there is  $1/L_m = 7.8 \times 10^5 \text{ cm}^{-1}$ . Thus the values of MEs shown in Fig. 11, although somewhat smaller than that for the cyclotron resonance, seem sufficient to make the corresponding optical transitions observable.

Next we turn to the peaks of higher wave vector  $q$  present in the electron wave functions, see Figs. 7, 8 and 9. These peaks should be observable by a resonant absorption of acoustic phonons. If the phonon dispersion is  $\mathcal{E}_{ph}(Q)$ , an absorption process will take place when the momentum conservation  $q_f - q_i = Q_{ph}$  and the energy conservation  $\mathcal{E}_f - \mathcal{E}_i = \mathcal{E}_{ph}$  are satisfied. This can occur for the same signs of  $q_i$  and  $q_f$  (which would require lower values of  $\Delta q$ ), as well as for the opposite signs of  $q_i$  and  $q_f$  (larger  $\Delta q$ ). The standard electron-phonon interaction via the deformation potential mechanism occurs for longitudinal phonons, so the latter should propagate along the growth direction of SL. The broadening of  $q$ -peaks, seen in Figs. 6, 7, 8, 9, should somewhat relax the momentum conservation which would facilitate the resonant phonon absorption. We emphasize again that the number of  $q$ -peaks in the electron wave functions available for the resonant transitions with phonons is twice as high for finite SLs as for "infinite" periodic structures. Transitions between electron states in different Brillouin

zones, known as the Umklapp processes, are known in the physics of 3D crystals. They contribute to electron scattering in transport phenomena and have usually a nonresonant character.

Coming back to finite SLs, it is difficult to imagine transitions between different  $q$ -peaks for the same electron energy since they would require excitations having relatively large momentum and vanishing energy. Such transitions could only participate in second-order excitations (for example in the Raman scattering), where the transitions to intermediate states require the momentum conservation but not the energy conservation. Also, one can imagine a resonant optic phonon emission accompanied by electron transitions between the states of different energy and momenta. Such phonon emission would cause an energy splitting of the upper electron state, similarly to the effects observed for the Landau levels of an electron in a magnetic field.

## V. SUMMARY

We describe electrons in finite superlattices treating the latter realistically as quantum wells and applying to them the fixed boundary conditions. We find that the electron wave functions are products of standing waves (of sine and cosine type) and periodic components. In classical terms, this corresponds to electrons bouncing back and forth. Our description is compared with the standard approach to electrons in periodic structures, based on the cyclic (Born-von Karman) boundary conditions, which are satisfied by running waves (Bloch states). We find that, while the total number of eigenenergies in a miniband is the same according to both treatments, the number of different eigenenergies is twice larger ac-

ording to FBCs. We also find that the wave vectors corresponding to the eigenenergies are spaced twice as densely according to FBCs as according to CBCs. An important difference between the two approaches is that a running wave is characterized by one value of the wave vector  $k$ , while a standing wave is characterized by a pair of wave vectors  $\pm q$ . Considering SLs with increasing number of QWs we follow formation of basic entities of periodic structures: energy bands, crystal momenta, and Brillouin zones. We find that one can characterize electron states by the crystal momentum beginning with  $N = 2$  QWs, the s-like shape of a miniband is formed beginning with  $N = 4$  QWs, but for a formation of a Brillouin zone edge more than  $N = 10$  QWs are needed. We calculate numerically the wave functions for finite SLs and then their Fourier transforms for increasing number of QWs in order to determine the predominant crystal momenta  $q$  involved in them. We find that the main  $q$  peaks are broadened, which is a direct consequence of the uncertainty principle. In addition to the main  $q_n$  peak, the FTs exhibit smaller peaks at  $q_n + G_i$  and  $-q_n + G_i$ , where  $G_i$  are reciprocal lattice vectors. This is similar to the common property of Bloch states, but in our case the number of high  $q$  peaks is twice higher. Finally, we consider experimental possibilities to observe the described properties of finite SLs with the use of photons and phonons.

## Acknowledgments

We acknowledge the financial support of Polish Ministry of Science and Higher Education through Laboratory of Physical Foundations of Information Processing.

- 
- [1] L. Esaki and R. Tsu, IBM J. Res. Dev. **14**, 61 (1970).
  - [2] D. L. Smith and C. Mailhot, Rev. Mod. Phys. **62**, 173 (1990).
  - [3] S. L. Altmann, *Band Theory of Metals*, (Pergamon, Oxford, 1970).
  - [4] G. Bastard, *Wave Mechanics Applied to Semiconductor Heterostructures*, (Les Editions de Physique, Les Ulis, 1996).
  - [5] R. A. Smith, *Wave Mechanics of Crystalline Solids*, (Chapman and Hall, London, 1961).
  - [6] C. Kittel, *Introduction to Solid State Physics*, (Wiley and Sons, New York, 1996).